



Erosion rates deduced from seasonal mass balance along the upper Urumqi River in Tianshan

Youcun Liu, F D Métivier, J Gaillardet, Baisheng Ye, P Meunier, C Narteau, E Lajeunesse, Tianding Han, L Malverti

► To cite this version:

Youcun Liu, F D Métivier, J Gaillardet, Baisheng Ye, P Meunier, et al.. Erosion rates deduced from seasonal mass balance along the upper Urumqi River in Tianshan. *Solid Earth*, 2011, 2, pp.283 - 301. 10.5194/se-2-283-2011 . hal-01499438

HAL Id: hal-01499438

<https://u-paris.hal.science/hal-01499438>

Submitted on 31 Mar 2017

HAL is a multi-disciplinary open access archive for the deposit and dissemination of scientific research documents, whether they are published or not. The documents may come from teaching and research institutions in France or abroad, or from public or private research centers.

L'archive ouverte pluridisciplinaire **HAL**, est destinée au dépôt et à la diffusion de documents scientifiques de niveau recherche, publiés ou non, émanant des établissements d'enseignement et de recherche français ou étrangers, des laboratoires publics ou privés.

Erosion rates deduced from seasonal mass balance along the upper Urumqi River in Tianshan

Y. Liu^{1,2}, F. Métivier¹, J. Gaillardet¹, B. Ye³, P. Meunier⁴, C. Narteau¹, E. Lajeunesse¹, T. Han³, and L. Malverti¹

¹Institut de physique du globe de Paris – Sorbonne Paris Cité, Université Paris Diderot, CNRS, UMR 7154, 1 rue Jussieu, 75238 Paris Cedex 05, France

²Key Laboratory of Water Environment and Resource, Tianjin Normal University, 393 Binshui west road, Tianjin 300387, China

³The States Key laboratory of Cryospheric Science, Cold and Arid Region Environmental and Engineering and Research Institute, Chinese Academy of Sciences 260 Donggang west road, Lanzhou, China

⁴Département de Géologie, UMR8538, CNRS, Ecole Normale Supérieure, 24 rue Lhomond, 75005 Paris, France

Received: 6 June 2011 – Published in Solid Earth Discuss.: 7 July 2011

Revised: 4 November 2011 – Accepted: 14 November 2011 – Published: 13 December 2011

Abstract. We report measurements performed during two complete flow seasons on the Urumqi River, a proglacial mountain stream in the northeastern flank of the Tianshan, an active mountain range in Central Asia. This survey of flow dynamics and sediment transport (dissolved, suspended and bed loads), together with a 25-year record of daily discharge, enables the assessment of secular denudation rates on this high mountain catchment of Central Asia. Our results show that chemical weathering accounts for more than one-third of the total denudation rate. Sediment transported as bed load cannot be neglected in the balance, given that sand and gravel transport accounts for one third of the solid load of the river. Overall, the mean denudation rates are low, averaging $46 \text{ t} \times \text{km}^{-2} \times \text{yr}^{-1}$ ($17\text{--}18 \text{ m Myr}^{-1}$). We furthermore analyse the hydrologic record to show that the long-term sediment budget is not dominated by extreme and rare events but by the total amount of rainfall or annual runoff. The rates we obtain are in agreement with rates obtained from the mass balance reconstruction of the Plio-Quaternary gravely deposits of the foreland but significantly lower than the rates recently obtained from cosmogenic dating of the Kuitun River sands, west of the Urumqi River. We show that the resolution of this incompatibility may have an important consequence for our understanding of the interplay between erosion and tectonics in the semi-humid ranges of Central Asia.

1 Introduction

Sediment transport in rivers remains an essential topic of research in earth sciences. Hydrographic networks shape landscapes and transport up to 90 % of eroded materials (Goudie, 1995). Knowledge of the dynamics of how matter is transferred is therefore essential for understanding the evolution of landscapes (Paola et al., 1992; Howard et al., 1994; Dietrich et al., 2003), especially mountainous landscapes in active tectonics regions (Métivier and Gaudemer, 1999; Lague et al., 2003). The potential role of erosion on the dynamics of a mountain range has gained increasing attention in recent years from the study of active mountain belts such as the Himalayas and Taiwan (e.g. Avouac and Burov, 1996; Whipple, 2009, and references therein). Therefore, it has become a key issue to assess rates of denudation at different time and space scales through the comparison between present day denudation rates and indirect estimates obtained from the study of sedimentary basin records or measurements of in situ-produced cosmogenic nuclides.

Here we use mass balance and hydrologic measurements to tackle two problems concerning erosion rates in mountainous environments: the relative importance of chemical versus mechanical weathering (Prestrud Anderson et al., 1997; Caine, 1992; Sharp et al., 1995; Smith, 1992; West et al., 2002, 2005; Schiefer et al., 2010), and the importance of the coarse fraction (bed load) in the estimate of mass budgets and mechanical denudation rates (Galy and France-Lanord, 2001; Gabet et al., 2008; Lenzi et al., 2003; Métivier et al., 2004; Meunier et al., 2006a; Pratt-Sitaula et al., 2007; Schiefer et al., 2010; Turowski et al., 2010).



Correspondence to: F. Métivier
(metivier@ipgp.fr)

The partitioning between solid and solute loads remains an issue in mountainous areas (West et al., 2002, 2005). In the Haut Glacier d'Arolla in the Swiss Alps, mechanical erosion seems more important than chemical denudation by orders of magnitude (Sharp et al., 1995). The exact contrary has been shown for the Green Lakes catchment in the Colorado Front Range by Caine (1992). There chemical denudation rates, although low, are an order of magnitude larger than mechanical denudation rates. In the Canadian Rockies, Smith (1992) also found that chemical denudation rates could be much more important than other mechanisms such as solifluction on the slopes. These large variations are often related to lithologic or biologic controls (Millot et al., 2002; Oliva et al., 1999), tectonic control (Riebe et al., 2001), agricultural land use (West et al., 2002), and glacial cover (Anderson et al., 2003). In mountainous settings, the importance of chemical weathering depends on the influence of the glacial cover, when present. Glacierized catchments have been shown to have significant weathering rates (Prestrud Anderson et al., 1997), yet these catchments are also often the place of a significant mechanical denudation.

Mechanical denudation in itself is still a matter of concern because the solid load is mostly restricted to the fraction of matter carried in suspension. The relative importance of the coarse fraction, also called bed load as the grains roll and saltate on the rough river bed, compared to the fine suspended fraction transported by mountainous rivers often remains obscure. Recent assessments have shown that bed load, which is seldom measured, could amount to a non negligible fraction of the total load transported in active mountain ranges (Galy and France-Lanord, 2001; Lenzi et al., 2003; Métivier et al., 2004; Meunier et al., 2006a; Pelpola and Hickin, 2004; Pratt-Sitaula et al., 2007; Schiefer et al., 2010; Wulf et al., 2010). Despite this, bed load is often simply assumed to be a given fraction of the suspended load without any further discussion.

We hereafter report a two-year survey on a braided stream in the Chinese Tianshan mountain range: the Urumqi River. We use this survey together with a 25-year record of discharge to perform a mass balance, derive erosion rates in a glacial catchment and discuss the respective contribution of mechanical and chemical weathering to denudation. We first describe the data acquisition (the complete dataset is available as Supplement), and discuss measurement issues. We then present the daily pattern of sediment transport during two consecutive summers (2005 and 2006). The results are then used to derive a daily mass budget. We show that the concentration of both dissolved and solid loads are highly correlated to discharge. Rating curves are then derived and used together with a 25-year record of daily discharge to estimate yearly fluxes of dissolved and solid material and the corresponding weathering rates. Finally, the results obtained are discussed and compared to existing longer-term measurements of denudation rates.

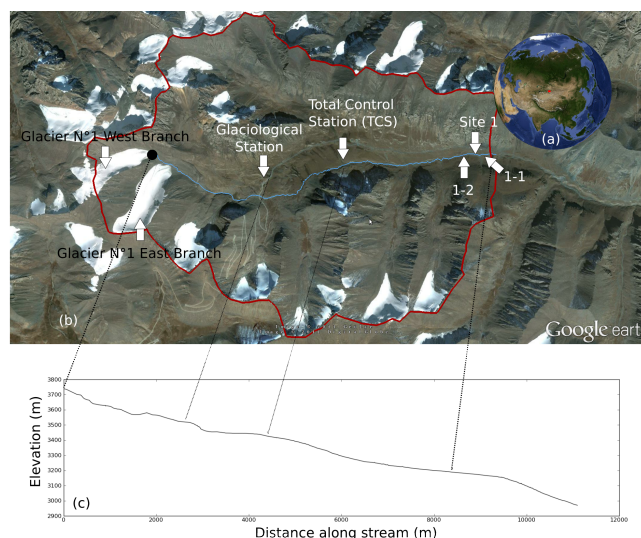


Fig. 1. Location map: (a) location of Tianshan and survey site, (b) satellite image and map of the Urumqi River drainage showing the sampling reach (Google Earth kml file available as Supplement), (c) kinematic GPS along the stream profile of the Urumqi River.

The mountains of Central Asia present an interesting counterpoint to the Himalayan orogeny or Taiwan accretion for the study of erosion and sediment transport. Although the elevation is high, the climate does not produce such intense events as monsoons or yearly typhoons. Precipitation is essentially orographic and of limited amplitude (Zhao et al., 2008). On average, only 450 mm yr^{-1} of rain falls over the Chinese Tianshan compared to the 2500 mm yr^{-1} of rain that falls over Taiwan. Glacial retreat is well on its way (Aizen et al., 1997; Ye et al., 2005) and the size and depth of the remaining Tianshan glaciers is much smaller than their Himalayan counterpart. Yet this region is the place of significant and active tectonics. Convergence between the Tarim block (Taklamakan Desert) and the Dzunggar block (Dzunggar or Junggar Desert) accounts for a non negligible fraction of the India-Asia convergence (Avouac et al., 1993; Avouac and Tapponnier, 1993; Wang et al., 2001; Yang et al., 2008). The Tianshan mountain range is therefore a place where it is possible to survey sediment transport, both dissolved, suspended and bed load, using conventional equipment (Métivier et al., 2004; Meunier et al., 2006a), while tackling questions of geodynamic significance (Avouac et al., 1993; Molnar et al., 1994; Métivier and Gaudemer, 1997; Charreau et al., 2011; Poisson and Avouac, 2004).

2 The Urumqi River

The dataset was acquired on the Urumqi River, a mountain stream located in the northeastern part of the Tianshan mountain range in China (Fig. 1, a GoogleEarth kml file is enclosed as Supplement). The river flows from south to north

and ends in a small reservoir in the Dzungar Basin. Tianshan is an intracontinental range that was reactivated during the Cenozoic in response to the India-Asia collision (Avouac et al., 1993; Molnar et al., 1994; Métivier and Gaudemer, 1997). It is located both in Kazakhstan, Kyrgyzstan and China, 2000 km north of the collision front. The range experiences north-south compressive shortening and accommodates approximately 40 % of the convergence (Avouac et al., 1993; Yang et al., 2008). The range extends for more than 2500 km and is bordered to the south and north by two internally drained sedimentary basins: the Tarim and Dzungar Basins, respectively. The Dzungar Basin covers an area of 130 000 km². The sedimentary infill is of alluvial, lacustrine and aeolian type. Water comes from the adjacent mountain ranges: Tianshan to the south, Altai to the north and east and Zhaiyier to the west. The Dzungar Basin records approximately 250 million years of sedimentary history. Deposits in front of the Tianshan range have experienced folding during Mesozoic and Cenozoic times (Chen et al., 2011; Hendrix, 1992; Jolivet et al., 2010). Folding was reactivated during the late Tertiary and Quaternary due to the northward propagation of deformation in the Tianshan. Deformation in the piedmont is still active. Incision and entrenchment of all streams flowing to the basin is one of the main features of late glacial morphology (Molnar et al., 1994; Poisson and Avouac, 2004). The Urumqi, like other rivers, has incised deeply into its alluvial fan and created well defined terraces.

The headwaters of the Urumqi River originate at 3600 m a.s.l. The river originates from a glacier known as Glacier No. 1 that flows from Tangger peak (Fig. 2). The stream flows for 60 km before it leaves the high range and enters its alluvial piedmont. The drainage of the Urumqi at the range front is 925 km². Hydrology is controlled by both orographic summer precipitation and glacial melting (Li et al., 2010; Ye et al., 2005).

The survey reported herein took place along a high mountain reach of the river (3200 m a.s.l.) in a U shaped glacial valley at a distance of 8 km from the headwater glaciers (Figs. 1, 2 and 3). The drainage area at the survey site is 45 km². This alpine landscape consists of poorly vegetated meadows, glacial tills and rock exposures. Rock outcrops consist of diorite, augen gneiss, schists and small outcrops of granite near the headwaters (Yi et al., 2002). There seems to be no limestone outcrop upstream of the survey site. Eventually, permafrost is present in the valley.

One of the advantages of surveying the Urumqi River lies in the existence of a large body of publications and studies on hydrology in this river due to the presence of the Tianshan Glaciological Station of the Chinese Academy of Sciences (e.g. Han et al., 2006; Lee et al., 2002; Li et al., 2006, 2010; Ye et al., 2003, 2005; Yi et al., 2002; Zhang et al., 2005; Zhao et al., 2008).

The river morphology at the sampling site varies from a wandering to a weakly braided gravel bed stream (Fig. 2). The median grain size is on the order of $D_{50} \sim 20$ mm and



Fig. 2. Channel morphology of the Urumqi River. The Urumqi River originates from the Tangger Glacier located on the northern flanks of the Tianshan range: (a) Site 1-2, view upstream on 16 May 2006 when the channel is dry. (b) Site 1-2 during the rise of the water level on 17 May 2006. (c) Site 1-1 on 16 May 2006, looking downstream. (d) Site 1-1 during the flood of 3 July 2006. (e) General view of the Urumqi glacial valley towards Tangger peak (in the back). (f) Source glaciers of the Urumqi River with moraines in the front.

$D_{90} \sim 160$ mm (Métivier et al., 2004). The bed is organized into patches and there is no developed armour (Figs. 2a–c). The mean annual temperature and precipitation measured at the Daxigou meteorological station near the sampling site are -5.1°C and 450 mm, respectively (Ye et al., 2005). At this location the river flows for approximately a five-month period between mid-May to mid-October, corresponding to the melt period. Flow is surveyed by the Tianshan Glaciological Station of the Chinese Academy of Sciences from May to September. About 90 % to 95 % of the annual flow occurs during these five months (Li et al., 2010). Based on the glacial runoff measured at the Number 1 glacier by the Chinese Academy of Sciences and on the total surface of the glaciers in the catchment, it is possible to estimate that about 40 % of the discharge at the sampling site comes from glacial melting whereas the remaining 60 % comes from precipitations (Li et al., 2010).

The measurements reported hereafter were performed at two different subsites approximately 130 m apart (Figs. 1, 2 and 3) and located approximately 2.5 km downstream of the

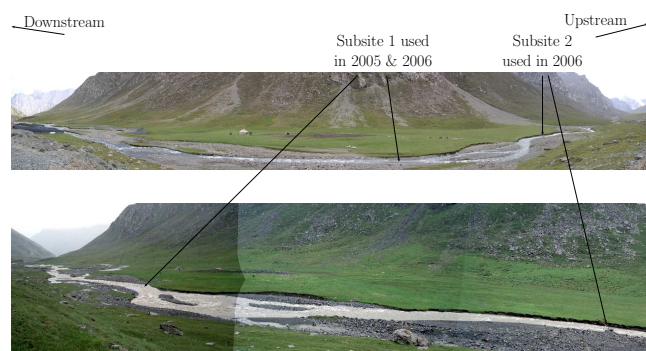


Fig. 3. Sampling sites in the glacial valley: site 1-1 was used during the years 2004–2006 whereas site 1-2 was only used in 2006 when a small iron bridge enabled sampling of the stream at high flows.

Total Control Station site of the Tianshan Glaciological Station (see Fig. 1 for location). Site 1-1, where measurements were made during the three years of survey, is located downstream of a confluence scour (Fig. 3). Site 1-2 is located under a small iron bridge that was constructed in 2006 on a straight reach of the river just upstream of site 1-1 (Fig. 3). We therefore have a double series of measurements in this area in 2006.

3 Data acquisition

3.1 Water sampling

Water samples were taken with a depth integrating USDH48 sediment sampler. Each sample was taken in the centre of the channel by an operator who manually lowered and raised the sampler at a constant velocity.

Samples were filtered through Nalgene filtration units using 0.45 μm filters within a couple of hours after being collected. The collection of samples for solute analyses started after 250 ml of river water was passed through the filter. Two vials were collected: one was acidified to $\text{pH} = 2$ for cation analysis, and the other one was kept non-acidified for anion and silicic acid measurements. Solute concentrations were measured in Paris by Dionex ion chromatography. For all cations and anions, the precision is better than 5 %. The concentration of bicarbonate ion HCO_3^- was deduced from cation and anion concentrations by electrical mass balance. Filters were dried in an oven at 60 °C and weighted to determine the solid mass of the suspended matter.

3.2 Bed load

Bed load measurements were made using a hand held pressure difference sampler. The opening of the sampler measured 0.3 by 0.15 m, the expansion ratio was 1.4, and the sampler was equipped with a 0.25 mm mesh bag. Given these dimensions, our sampler should have the same properties as

a Toutle river sampler (Diplas et al., 2008). These samplers were devised following discussions on the problems associated with using samplers with large pressure differences such as the Helley-Smith sampler (Hubbell, 1987; Thomas and Lewis, 1993; Diplas et al., 2008). Sampling efficiency of the Toutle river sampler ranges between 80–116 % (Diplas et al., 2008) so that the measurements obtained are on average likely to be good estimates of the true fluxes. On average, the sampling duration was 120 s per sample. Each individual sample was weighed. Liu et al. (2008), through a comparative analysis, have shown that cross-sectional sampling could lead to an order of magnitude bias in the flux measured. They furthermore showed that cross-section samples did not enable us to catch the full range of flow conditions. We therefore did not follow the cross-section average sampling procedure. Yet it is possible to integrate the local transport rates in order to calculate the bed load flux passing through the section. We adopt this procedure here. Bed load catches were then dried and sieved in order to study the fractional transport of sediment (Liu et al., manuscript in prep.). The average ratio between the dry and wet mass was found to be 0.86 for the Urumqi River.

There has been much debate on bed load sampling techniques, especially using portable samplers (Bunte and Abt, 2005; Vericat et al., 2006; Bunte et al., 2008; Diplas et al., 2008). We therefore found it interesting to compare measurements performed at two subsites separated by 200 m. The measurements were not concurrent but were made sufficiently close to one another so that the discharge did not change significantly (see discussion on velocity measurements). Individual local transport rates were integrated over the wetted perimeter to obtain the mass flux passing the section at each subsite. The measurements were then compared. Figure 5 shows this result. A clear trend is observed and the majority of the measurements are comparable within a factor of two. Almost all bed load rates are comparable within a factor of 5.

The observed variations can be related to the sampling technique, the inherent stochastic nature of individual grain movement or local degradation or aggradation waves. Nevertheless, it is interesting to note that the majority of our measurements of bed load rates collapse within a factor of 2. This indicates that the sampling technique, within its limitations (Ryan and Porth, 1999; Bunte and Abt, 2005; Vericat et al., 2006; Diplas et al., 2008), seems both robust and reproducible. It also suggests that, on average, bed load transport remains constant along the reach.

3.3 Flow velocity and discharge

For each bed load measurement, a velocity profile was made at the same location. Velocity was measured with an OTT C20 mechanical velocimeter (Métivier et al., 2004; Meunier et al., 2006b; Liu et al., 2008, 2010). Between one and five individual measurements of the velocity were made,

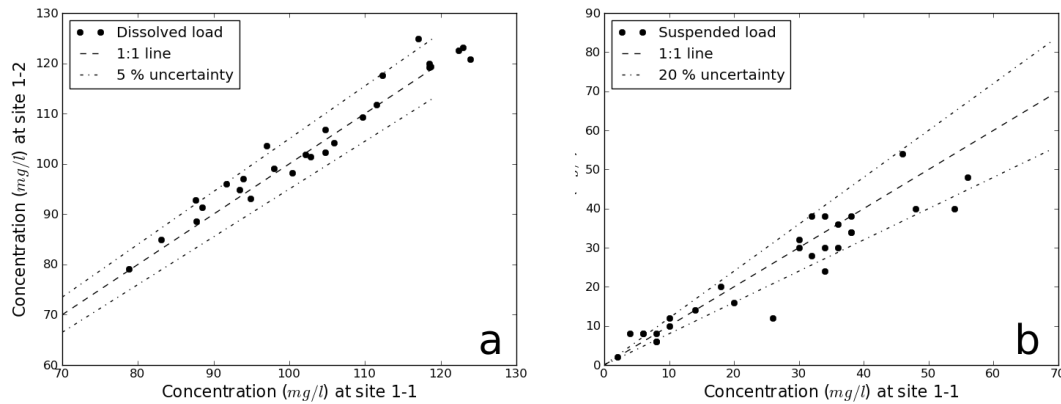


Fig. 4. Reliability of measured fluxes: **(a)** Comparison between measured concentrations in major ions in the glacial valley at sites 1-1 and 1-2. **(b)** Comparison between measured suspended concentrations at both subsites. The dashed line represent perfect agreement, and the dotted-dashed lines represent 5 % deviation from 1:1 agreement for the dissolved load and 20 % deviation for the suspended load.

depending on flow depth. Each individual measurements gives the velocity averaged over 60 s.

Average flow velocity was calculated by simple discrete integration following:

$$u = \frac{1}{h} \int_0^h v(z) dz \simeq \frac{1}{h} \sum_{i=1}^{i=n-1} 0.5(v_{i+1} + v_i)(z_{i+1} - z_i) \quad (1)$$

where $v_i(z_i)$ is the individual measure of the velocity (in m s^{-1}) of the i^{th} point taken at depth z_i where the flow depth is h . n is the number of measurement points. Based on continuity assumption, we assume that the velocity at the bed is zero. Discharge is then calculated by transverse integration of the velocity; hence,

$$Q = \int_0^W \int_0^h v(y, z) dy dz = \int_0^W u(y) dy \quad (2)$$

$$\simeq \sum_{j=1}^{j=m-1} 0.5(u_{j+1} + u_j)(y_{j+1} - y_j)$$

where $u_j(y_j)$ is the average velocity of the j^{th} point taken at a distance y_j from the bank of the stream with width W . m is the number of measurement points. Here again continuity implies that the average velocity u is zero at the banks. This technique was successfully used by Meunier et al. (2006a) to study the dynamics of flow in a proglacial mountain stream in the French Alps. This technique, although time consuming, has advantages compared to other gaging techniques (see Sanders, 1998). First, it does not necessitate any assumption about the form of the velocity profiles to derive the average flow velocity and discharges. Second, it can be used to derive shear stress distributions on the bed and friction coefficients.

3.4 Relevance of data acquisition

To summarize, the survey of the Urumqi River was performed using acquisition and processing procedures that are

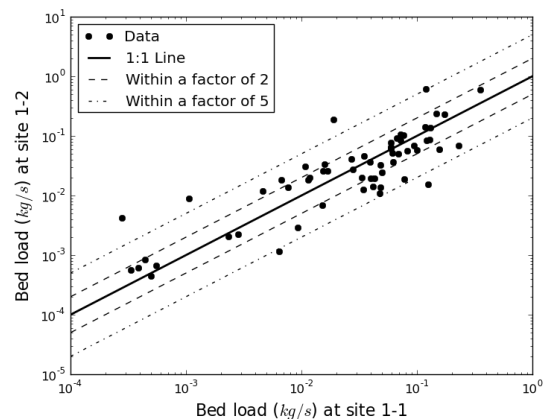


Fig. 5. Comparison between the bed load rates measured at sub-sites 1 and 2 on the Urumqi River during the summer 2006. The solid line corresponds to perfect agreement, the dashed lines correspond to 2:1 and 1:2 ratios, respectively and the dotted-dashed lines correspond to 5:1 and 1:5 ratios uncertainty envelope.

comparable to classical procedures used by other researchers (Ashworth et al., 1992; Meunier et al., 2006a; Habersack et al., 2008) on several field sites. Our dataset, spans several flood seasons and includes both hydrology and flow velocity measurements, sediment information (bed load and suspended load) and chemical composition. Altogether, 194 gagings and coeval sediment sampling were performed on the river during 2005 and 2006. The dataset is available in electronic Supplement.

Repeated sampling at two geographically close subsites in 2006 allows for a direct estimate of the reproducibility of our measurements. As expected, dissolved concentrations are the most reproducible measurement. Concentrations measured at the two subsites are equivalent within 5 %. Discharge and suspended concentrations are found to be consistent within 20 % (Fig. 4). The larger uncertainty may be related to effects

such as section topography, sampling time (it takes approximately 30 to 45 min to perform a gaging) and spacing between points (density of the measurements). Sampling time is probably the most important factor. Given the uncertainty related to using mechanical propellers and the fact that discharge varies on a diurnal basis due to glacial melting, Fig. 6 clearly validates the measurements performed.

Bed load, as discussed above, is the least reproducible quantity measured. Most rates are consistent within a factor of 5 and a little more than half within a factor of 2. Again, this is perhaps due to the sampling procedure, bed composition or local topography (width, depth and slope), and the fact that bed load is by essence a local phenomenon that is difficult to sample and integrate over a section (Liu et al., 2008).

In order to simplify the analysis, a composite series was made for 2006. For the days on which concurrent measurements were performed at the two subsites, we averaged the resulting values. For the days on which only one section was surveyed, we used the available data. Thus, unless explicitly mentioned, the 2006 dataset is a composite sample of the measurements performed at the two subsites.

4 Analysis of the results

Figure 7 shows the evolution of the total load measured in the Urumqi River together with the repartition of this load into solute, suspended and bed loads. The first striking feature of mass transport in the Urumqi River is the importance of dissolved load. Solute transport accounts for more than 80 % of total mass transport during low flows. During the summer, its contribution diminishes but remains of primary importance oscillating between 20 and 60 % of the total mass carried by the stream. The total dissolved flux measured in 2005 and 2006 accounts for 41 and 54 %, respectively, of the total flux carried by the river during the summer months.

The second striking feature is the relative importance of bed load transport. Bed load is of the same order of magnitude as suspended load. Suspended load seems to become predominant only during the largest floods. In the next two paragraphs we will first analyse solid transport at the measurement site; then we will try to assess the fraction of the dissolved contribution to the weathering of the catchment.

4.1 Solid transport

Figure 8 shows daily discharge measurements together with daily bed load and suspended load fluxes. Local bed load measurements made with a hand held sampler were integrated over the section to obtain the bed load flux passing through the section. The average concentration of suspended load obtained from depth integration at the section centre was multiplied by the discharge to calculate the flux of suspended matter.

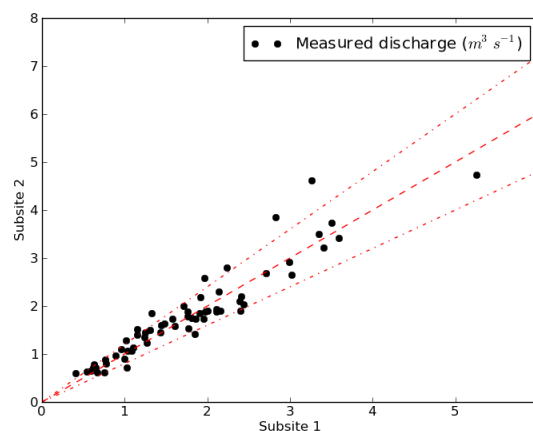


Fig. 6. Comparison between discharge measured at sites 1-1 and 1-2 on the Urumqi River during the summer of 2006. The dashed line corresponds to perfect agreement and the dotted lines correspond to a 20 % uncertainty envelope.

Bed load movement is not marginal in the Urumqi River. Significant transport occurs throughout the flow season. Bed load accounts for 29 and 38 % of the total solid load in 2005 and 2006, respectively. It is of the same order of magnitude as suspended load during high flows and cannot be neglected. The main difference comes from the existence of suspended sediment transport throughout the flow season, whereas the increase of bed load transport is correlated to the increase of discharge during the summer months.

Measurements made at sites 1-1 and 1-2 during the summer of 2006 clearly exhibit the same history of sediment transport. Measurements during the highest floods were particularly challenging. During these high flows, bed load could not be sampled at positions where flow was the fastest but only near the banks in lower flow velocity zones. This most probably leads to a severe underestimation of true fluxes and probably explains why the highest water levels are not correlated to the highest bed load rates. Figure 9 shows the percentage of daily fluxes above a given value (inverse CDF) for the years 2005 and 2006. Daily rates of more than 2 t are recorded during half of the season. Values of 10 t are exceeded between 13 and 25 % of the time, i.e. between 7 and 12 days during the two first months of summer.

During the years 2005 and 2006, a remarkable and unexplained picture emerges. The flow season is marked by an initial peak discharge that occurs during the first ten days of July. During this initial period flooding reaches its maximum. The hydrograph then decays a bit and goes back up again with several flood peaks until the end of August when the flow goes below $1 \text{ m}^3 \text{ s}^{-1}$. The bed load exhibits the same trend but the magnitude of sediment transport is not significantly larger than the following transport events that occur during mid-July until the end of August, as if larger flows were needed to remobilize the bed at the beginning of the season.

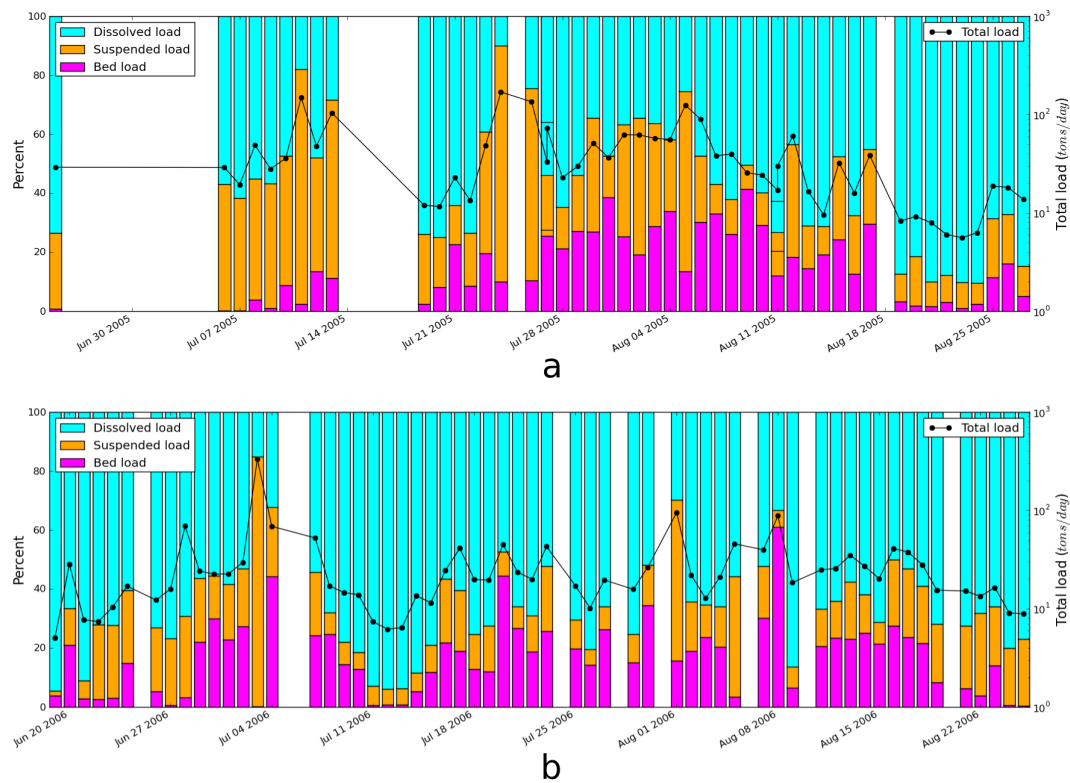


Fig. 7. Mass flux balance: (a) Total flux of mass both dissolved and solid measured in the Urumqi River during the summer of 2005 together with the proportion of dissolved load, suspended load and bed load (coloured cumulative histograms). (b) Same for 2006.

Table 1. Average solute concentrations (in $\mu\text{mol l}^{-1}$) measured in the Urumqi River (this study), in the snowpack (Williams et al., 1995) and in the precipitation (Zhao et al., 2008). Averages are volume-weighted for both precipitation and river fluxes.

Element	River	Rainfall	Snowpack
Na ⁺	59.7	19.0	9.7
K ⁺	25.4	4.0	1.2
Mg ²⁺	77.3	9.1	3.0
Ca ²⁺	434.9	87.1	26.2
F ⁻	11.9	–	–
Cl ⁻	33.3	16.5	9.9
NO ₃ ⁻	44.9	9.6	5.7
NH ₄ ⁺	–	25.2	–
SO ₄ ²⁻	171.6	26.5	8.1
HCO ₃ ⁻	676.2	61.7	50.2
SiO ₂	47.6	–	0.4

4.2 Dissolved load

Table 1 reports the volume-weighted average concentrations in the Urumqi River in both the rainfall (Zhao et al., 2008) and the snowpack (Liu et al., 1995; Williams et al., 1995). Table 2 reports the minimum and maximum values of the ra-

tios X/Cl where X is a given element. Figure 10 shows the chloride normalized ratios $\text{Ca}^{2+}/\text{Cl}^{-}$ versus $\text{Na}^{+}/\text{Cl}^{-}$ for the two years of measurements. Examination of the data shows that the dissolved load of the Urumqi River is dominated by three chemical species: Ca^{2+} , SO_4^{2-} and HCO_3^{-} . Bicarbonate is responsible for half of the total load. The total dissolved load fluctuates from 50 mg l^{-1} to 135 mg l^{-1} , with the higher concentrations associated to the lowest water discharges. Ca^{2+} concentrations are particularly well correlated with the total solute load. The concentrations reported in this study are consistent with previous analyses from Williams et al. (1995) in river samples from the snowmelt period. Rainwater and snow (from snowpacks) were also reported by Williams et al. (1995), Liu et al. (1995) and Zhao et al. (2008). While the former have shown that the chemistry of the snowpack has little influence on the water chemistry during the first days of river flow in May, the latter have shown that the atmospheric contribution to the river chemistry could not be neglected. The assessment of rain contribution to the river is important and can be estimated based on the Cl^{-} concentration. Chloride occurs in plutonic rocks as a trace element in a couple minerals. Yet compared to the amount of chloride delivered by rainwater, the input of lithogenic chloride is not significant. Furthermore, the geology of the basin does not indicate the occurrence of evaporite

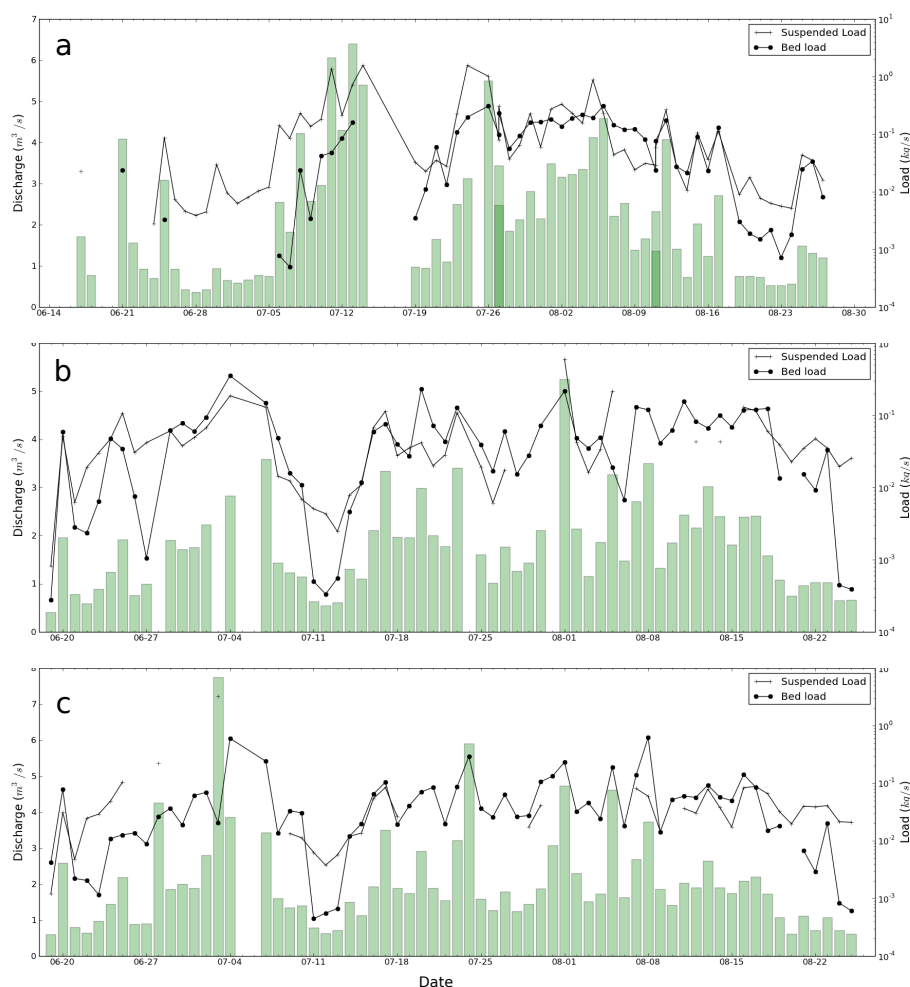


Fig. 8. Daily measurement of discharge, suspended load and bed load transport rates along the Urumqi River in its glacial valley. (a) site 1-1 in 2005, (b) site 1-1 in 2006, (c) site 1-2 in 2006.

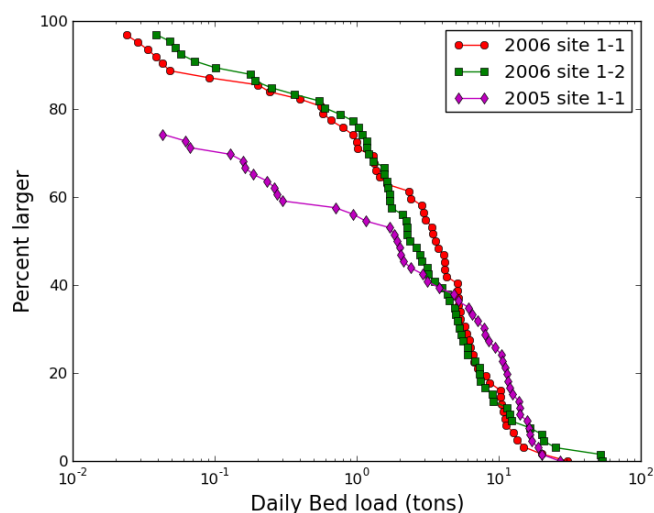


Fig. 9. Distribution of bed load fluxes: Proportion of daily bedload exceeding a given value in tons per day.

rocks. Therefore, it is reasonable to assume that the Cl^- in the dissolved load is derived entirely from the atmosphere. This is consistent with the average Cl^- concentration in the rain (Zhao et al., 2008) and an evapotranspiration factor of 2 (estimated by Zhang et al., 2005). It is therefore possible to use the chemical composition of the rainwater and the snow-pack to correct the riverine concentrations from atmospheric inputs. It is important to note that the rainwater from the Tianshan mountains is highly concentrated compared to the world average (Berner and Berner, 1996). This feature is attributed by Zhao et al. (2008) to the leaching of atmospheric dust derived from the Takimakan desert. The origin of chloride is probably desertic evaporite formations. Zhao et al. (2008) have shown that, in the glacial valley, winds could carry a large amount of dusts from the Taklimakan Desert, south of the range, and that this desert was probably the main source of NaCl present in the summer orographic precipitation. The dissolved load of the river is thus expected to be a mixing between solutes derived from the rocks between the

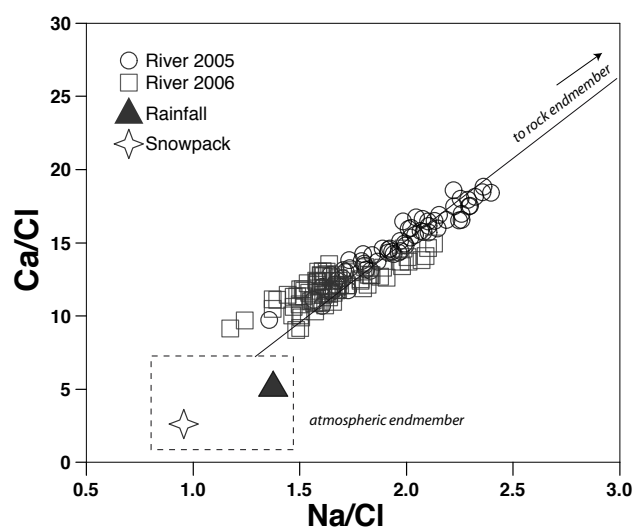


Fig. 10. Mixing diagram showing that the water samples from Urumqi River can be seen as a mixing between two endmembers: precipitation and water derived from a water/rock interaction within the drainage basin. Elemental ratios are not sensitive to evaporation processes. Note that 3 unexplained outlying points out of 134 are not shown on the figure but are available in the dataset.

Table 2. Minimum and maximum ratios of the chemical element concentrations normalized to Cl^- both in the rainfall (Zhao et al., 2008) and the Urumqi River (this study).

Ratio	Rainfall		River	
	Min	Max	Min	Max
Na^+/Cl^-	1	1.4	1.2	2.5
K^+/Cl^-	0.12	0.27	0.4	1.2
$\text{Mg}^{2+}/\text{Cl}^-$	0.25	0.45	1.5	3.5
$\text{Ca}^{2+}/\text{Cl}^-$	2	5	8	20
$\text{SO}_4^{2-}/\text{Cl}^-$	0.8	1.8	3	10
$\text{NO}_3^-/\text{Cl}^-$	0.4	0.6	0.8	2.7
$(\text{NO}_3^- + \text{NH}_4^+)/\text{Cl}^-$	1.5	2	–	–

drainage basin and rainwater. In Table 2, we show the minimum and maximum values of the Cl^- normalized ratios in the rainwater and Urumqi River for all cations and silica.

Na^+ , Ca^{2+} , Mg^{2+} and K^+ are enriched in the river compared to the rain and most probably derive from silicates (Na^+ , Mg^{2+} , K^+), and carbonates (Ca^{2+}). In Fig. 10, $\text{Ca}^{2+}/\text{Cl}^-$ and Na^+/Cl^- have been plotted for the two years of measurements; the straight line indicates a mixing between two main endmembers, which are likely to be the atmospheric input on one hand and a rock weathering endmember on the other hand. The relative enrichment in Ca with respect to Na for this latter endmember clearly indicates a carbonate weathering source (Negrel et al., 1993). Similar binary mixing relationships can be found using the different elemental ratios. The Urumqi River Basin is essen-

tially a silicate-dominated basin according to the geology, and it would be surprising to find a significant contribution of carbonate weathering. We attribute this significant carbonate contribution either to the contribution of carbonate dust derived from dry atmospheric deposits or to the contribution of disseminated carbonate minerals present in the bedrocks. Outcrops of carbonate rocks are described nearby by Williams et al. (1995), though apparently not upstream of the survey point (Yi et al., 2002), and a number of papers describing river water composition in high physical erosion regimes have noticed that even silicate draining waters can be influenced by carbonate dissolution (e.g. Anderson et al., 2003; Jacobson and Blum, 2000). This peculiarity is attributed by these authors to the contribution of disseminated calcite in the granitic rocks whose weathering is facilitated by glacial abrasion and the rapid production of fresh mineral surfaces by glaciers.

The $\text{SO}_4^{2-}/\text{Cl}^-$ ratio of the river samples is much higher in the river than in the rainfall. This clearly suggests that a source of sulphate is present in the drainage and that sulphate ions have to be included in the erosion budget. Sulfur oxidation could probably be a good candidate for this. This internal (rather than anthropogenic pollution) origin of sulphate is confirmed by the $\delta^{34}\text{S}$ values found by Williams et al. (1995) in the river waters. In particular, it seems that the possibility of the transport of dust particles from the steel mill located downstream in the town of Houxia or from Urumqi is low. Oxidative weathering of pyrite has been described in many places to be a significant source of sulphuric acid and thus of acidity. For example, Anderson et al. (2003) have shown that in glacierized catchments from Alaska, oxidative weathering of pyrite and carbonate weathering are the two over-riding mechanisms explaining the water chemistry. The global importance of carbonate weathering by sulphuric acid is a global feature that has also been recently documented in southern China, Taiwan or the Mackenzie River Basin by Calmels et al. (2007, 2011). The $\text{NO}_3^-/\text{Cl}^-$ ratio presents an interesting case. This ratio is higher in the river compared to the rainfall, but NH_4^+ is also present in the rainfall. If we calculate the ratio $(\text{NO}_3^- + \text{NH}_4^+)/\text{Cl}^-$ and compare it to the $\text{NO}_3^-/\text{Cl}^-$ measured in the river, the values become comparable. It is therefore possible that bulk nitrogen has an atmospheric origin and that nitrification occurs in the soil that transforms NH_4^+ into NO_3^- . This reaction provides an additional source of acidity available for chemical weathering. Finally, the rest of acidity is provided by carbonic acid and can be calculated based on the excess of bicarbonate in the river samples. On average, in the upper Urumqi River, the amount of protons derived from sulphuric acid is equivalent to that provided by soil carbonic acid. In a weathering mass budget perspective, bicarbonate that is of atmospheric origin does not have to be taken into account. In order to calculate the contribution of atmospheric inputs to the river chemistry, the volume-weighted mean annual chemistry of rainfall

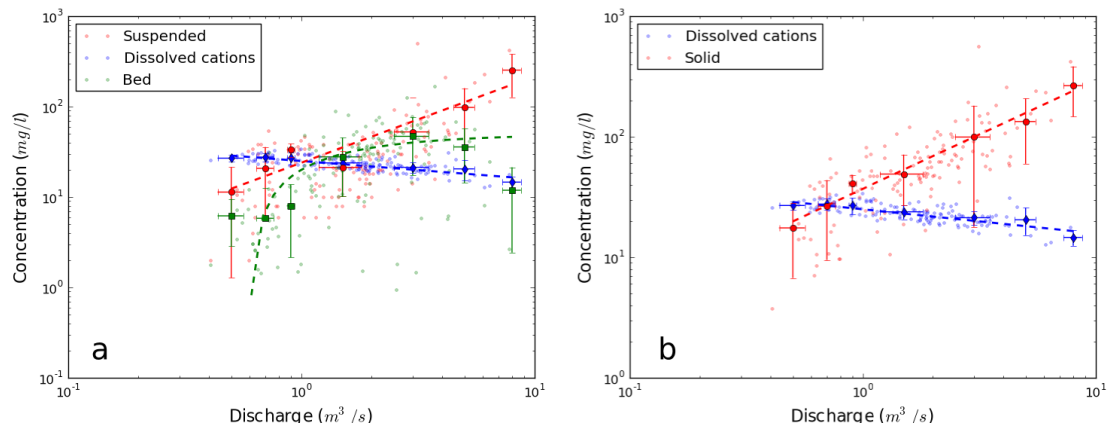


Fig. 11. Weathering and erosion: **(a)** correlation between the concentration and discharge for the weathering load, suspended load and bedload. **(b)** Correlation between chemical weathering concentrations and total solid concentrations versus discharge in the Urumqi River. Small points represent individual measurements, squares represent binned averages and dashed lines correspond to fitted trends.

collection in the glacial valley, 2 km upstream from our measurements by Zhao et al. (2008), was used.

$$[X]_{\text{cyclic}} = [\text{Cl}^-]_{\text{river}} \cdot \left(\frac{X}{\text{Cl}^-} \right)_{\text{rain}}, \quad (3)$$

where $[X]_{\text{cyclic}}$ is the contribution of rainfall for a given element X (Millot et al., 2002; Calmels et al., 2011). Atmospheric contribution was calculated for all the cations plus SO_4^{2-} (oxygen is not taken into account in the final balance as it comes from atmospheric CO_2). Half of the corresponding HCO_3^- content comes from the weathering of carbonates and was eventually taken into account (under the form CO_3^{2-}).

We assume that all Cl^- is of atmospheric origin and we therefore apply the mean annual chemistry of the rainfall correction to the 2005 and 2006 river samples. A significant atmospheric contribution is found for the Cl^- , Na^+ and Mg^{2+} ions, whereas Ca^{2+} , Si , K^+ and SO_4^{2-} are essentially derived from chemical weathering. The proportion of HCO_3^- derived from the bedrock was calculated based on the electrical balance:

$$\text{HCO}_3^-_* = 0.5 \left(2\text{Ca}^{2+}_* + \text{Na}^+_* + \text{K}^+_* + 2\text{Mg}^{2+}_* - 2\text{SO}_4^{2-}_* \right), \quad (4)$$

where $*$ denotes atmospheric correction. In the rest of the paper, dissolved concentrations, unless specifically stated, correspond to the fraction that comes from weathering in the catchment.

5 Mass balance and erosion rates

5.1 Rating curves for dissolved and solid concentrations

From our measurements it is possible to look for a relationship between discharge and concentrations both dissolved and solid. Figure 11 shows these results. Figure 11a shows the evolution of the chemical weathering, suspended and bed

load concentrations, respectively. Together with the raw data we show the binned averages (larger points). Binning is a simple averaging technique used to reduce noise from raw datasets (Kuhnle, 1992). The bed load concentration is calculated by the ratio of measured bed load fluxes (Q_b), to their measured discharge (Q_w),

$$C_b = \frac{Q_b}{Q_w}. \quad (5)$$

The average value for bed load transport at high flows is low and probably irrelevant because at high flows we were not able to sample the section evenly. The place of the highest flow (hence highest load) could not be sampled, leading to a severe underestimation of the fluxes. Apart from this bad value for bedload at high discharges, the picture that emerges is coherent. There is some scatter in the raw data points. Scatter is expected due to the measurement uncertainties discussed above and it is expected to be much larger for bed load than for suspended load and dissolved load. Despite this scatter, the average values exhibit clear trends. The bed load concentration rises from a threshold at around $0.6 \text{ m}^3 \text{ s}^{-1}$ to a constant value of around 50 mg l^{-1} . Hence, bed load fluxes become proportional to discharge. This type of evolution has already been noted by Mueller and Pitlick (2005) and Pitlick (2010) for rivers in Colorado. Suspended and chemical loads exhibit opposite power law trends, with a chemical concentration that slowly diminishes with increasing discharge whereas the suspended concentration increases with discharge. As noted earlier, for a significant range of discharges, all three loads are of the same order of magnitude. For small discharges, the chemical load becomes the dominant form of mass transport, whereas the suspended load becomes the dominant form of mass movement for large floods. The bed load evolves from a minimal contribution at low discharges to a median contribution at high flows. For a

characteristic discharge of about $1 \text{ m}^3 \text{ s}^{-1}$, all the concentrations are approximately equal.

Given these correlations and the related measurement uncertainties and in order to simplify the analysis and the mass balance presented herein, we added the bed load and the suspended load together to calculate a total solid load concentration

$$C_{\text{solid}} = C_s + C_b, \quad (6)$$

that can be compared to the chemical concentrations (Fig. 11b). As for Fig. 11a, the correlations are evident and can be fitted using simple power laws according to

$$C_{\text{dissolved}} = 40 Q^{-0.2}, \quad R^2 = 0.76 \quad (7)$$

and

$$C_{\text{solid}} = 37 Q^{0.9} \quad R^2 = 0.96. \quad (8)$$

The prefactors in Eqs. (7) and (8) correspond to the value of concentration at the characteristic discharge of $1 \text{ m}^3 \text{ s}^{-1}$. This discharge therefore corresponds approximately to an inversion in the relative importance of the loads: below $1 \text{ m}^3 \text{ s}^{-1}$, chemical weathering makes up the dominant component of mass transport; whereas above $1 \text{ m}^3 \text{ s}^{-1}$, the solid load becomes the dominant mass transport mechanism.

Finally, it is interesting to note that the correlation obtained for the dissolved load of the Urumqi River compares closely to the correlations found by Godsey et al. (2009) for rivers in the United States. The reasons for this nearly chemo-static (the concentration does not depend on discharge) behaviour where the concentration follows a power law dependence on discharge with a small negative (~ 0.2 – 0.25) exponent are still debated (Godsey et al., 2009; Devauchelle et al., 2011). However, at least in the case of the Urumqi River, the relatively low value of the exponent shows that the chemical composition is not diluted at high discharge.

5.2 Return period of floods in the Urumqi River

Recently, Schiefer et al. (2010) studied the pattern of sediment yield in a montane catchment of British Columbia. They showed that extrapolation of short-term surveys to estimate long-term denudation rates could be biased if the hydrologic regime, especially its variability, was not properly considered. This question was also raised by Wulf et al. (2010) in an analysis of the magnitude frequency distribution of rainfall in the northwest Himalays and the correlative importance of rare extreme events on the sedimentary budget of the Baspa River. We address this problem here by studying the magnitude frequency distribution of the discharges measured along the Urumqi River.

Upstream of our survey site, the Glaciological station of the Academy of Sciences maintains a hydrologic station where daily discharge is being measured four times a day during five months each year, from May to September (Li

et al., 2010). Although there may be some small flow after September (more rarely before May), these daily measurements (Fig. 12a) catch most of the discharge of the river. Our record extends from 1983 until 2007; only the year 1996 is characterized by a strong lack of data.

On 15 July 2005, the largest flood recorded in the valley occurred with a discharge of $9.56 \text{ m}^3 \text{ s}^{-1}$. This flood has a Weibull return period of 25 years, i.e. the length of the record. In order to assess its possibly larger return period, we performed a classical return period assessment using both lognormal and Gumbel distributions (Bennis, 2007). The results are shown in Fig. 12b–c. Both distributions predict all the maximum yearly discharges well except for the largest. The Gumbel distribution predicts that the flood observed in 2005 should occur once every 125 years, whereas the lognormal distribution predicts a return period of 377 years. Even if these return frequencies may be overestimated, this analysis shows that the 2005 flood most probably has a large return period – on the order of a century.

We could not sample this flood because the road was dangerous due to the rainfall, but we sampled floods of more than $7 \text{ m}^3 \text{ s}^{-1}$, which is obviously not orders of magnitude different from $10 \text{ m}^3 \text{ s}^{-1}$. Hence, there is no grounded reason why the concentration of material should exhibit a special trend for this special flood. Therefore, we can safely argue that the correlation obtained with our survey is robust in the sense that it holds for the entire range of possible discharges at the centennial time scale.

5.3 Influence of daily fluctuations

In order to derive daily denudation rates, we couple the discharge-concentration relationships (7) and (8) together with the daily mean discharge. One can argue that because of glacial melting the Urumqi River experiences a significant variation in terms of the discharge during each 24 h cycle. Because of the exponents of (7) and (8), this influence can be shown to be negligible. For simplicity's sake, let us assume that the hydrograph presents a symmetrical triangular shape with a rising and a falling limb of $T = 12$ hours each. The instantaneous discharge is defined according to

$$Q(t) = \left(\frac{Q_{\text{max}} - Q_{\text{min}}}{T} \right) t + Q_{\text{min}} \quad t \leq T, \quad (9)$$

$$Q(t) = \left(\frac{Q_{\text{max}} - Q_{\text{min}}}{T} \right) (2T - t) + Q_{\text{min}} \quad t > T, \quad (10)$$

where $Q(t)$ is the instantaneous discharge as a function of time t , Q_{max} and Q_{min} the maximum and minimum daily discharges. The average daily discharge is then $\langle Q \rangle = 0.5(Q_{\text{max}} + Q_{\text{min}})$. Assuming that the minimum discharge (at sunset) is negligible compared to the maximum discharge, equations 9 and 10 become

$$Q(t) = \left(\frac{Q_{\text{max}}}{T} \right) t \quad t \leq T, \quad (11)$$

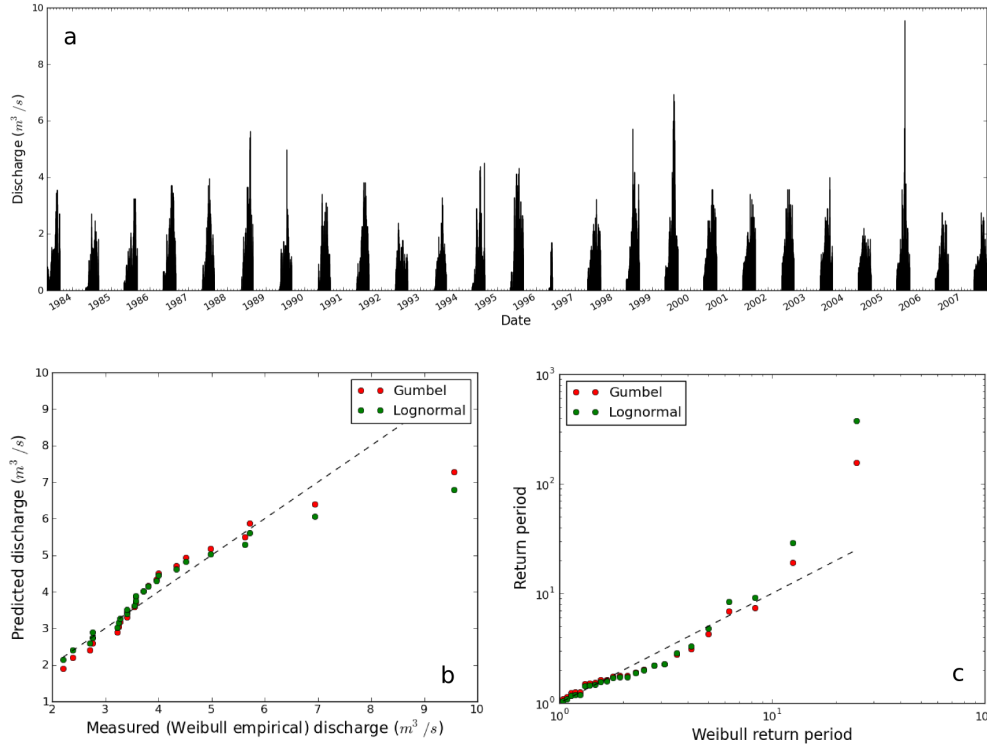


Fig. 12. River hydrology (a) Daily hydrograph of the Urumqi River during 25 years. (b) Comparison between the measured (Weibull empirical) and the predicted discharge using a lognormal or a Gumbel probability distribution. (c) Comparison between the Weibull empirical return period and the lognormal or Gumbel return periods for the Urumqi River.

$$Q(t) = \left(\frac{Q_{\max}}{T} \right) (2T - t) \quad t > T. \quad (12)$$

We then have $\langle Q \rangle \sim 0.5 Q_{\max}$. Using the relationships (7) and (8) between the mass concentration and discharge together with (11), we can then calculate the mass flux $q_{s,full}$ transported during the rising limb of the hydrograph (the same can be performed for the falling limb using (12)). For solid load, equations (8) and (11) lead to

$$q_{s,full} = C_{solid} * Q = 37 Q^{1.9} = 37 [(Q_{\max}/T)t]^{1.9}. \quad (13)$$

The mass $M_{s,full}$ that has been transported during a half cycle T is then

$$M_{s,full} = \int_0^T q_s dt = \int_0^T 37 [(Q_{\max}/T)t]^{1.9} = 37 Q_{\max}^{1.9} T / 2.9. \quad (14)$$

In the case where $Q = 0.5 \langle Q_{\max} \rangle$ equation (14) becomes

$$M_{s,av} = 37 (Q_{\max}/2)^{1.9} T. \quad (15)$$

The ratio of (14) and (15) leads to $M_{s,full}/M_{s,av} \sim 1.3$. In the case of dissolved budgets the ratio of these volumes is $M_{d,full}/M_{d,av} \sim 0.96$.

As these ratios are close to 1, in the case of the Urumqi River, we conclude that the use of average daily discharge to calculate the solute and solid transport is relevant.

5.4 Denudation rates

Figure 13 show the “weathering” budget for the 25-year period. The 25-year average values are $\sim 17 \text{ t} \times \text{km}^{-2} \times \text{yr}^{-1}$ for chemical weathering and $\approx 29 \text{ t} \times \text{km}^{-2} \times \text{yr}^{-1}$ for mechanical erosion. This gives a total of $46 \text{ t} \times \text{km}^{-2} \times \text{yr}^{-1}$ of erosion on the upper catchment of the Urumqi River. The catchment of the upper reach is mainly composed of diorites, granodiorites, and schists. Assuming an overall density of $2.65 \text{ t} \times \text{m}^{-3}$, our estimate of the mechanical and chemical weathering corresponds to an average denudation rate of approximately $17\text{--}18 \text{ m Myr}^{-1}$. As discussed earlier, the chemistry of the cations is dominated by the presence of Ca^{2+} and hence, by the weathering of carbonates. The source inside the basin is still a problem. Available geologic maps, such as the one provided by Yi et al. (2002), mention carbonate outcrops but not inside the area drained by our samples. It is therefore possible that the weathering of carbonates comes from the weathering of trace amounts of bedrock carbonates as shown by Blum et al. (1998) for the Raikhot catchment in the Himalayas. It is also possible that a significant Ca source can be found in the calcite veins deposited by fluid circulation during metamorphic events.

Recent hydrological analyses all lead to the conclusion that, due to global change, runoff is increasing together with temperature and rainfall. The average rise in air temperature

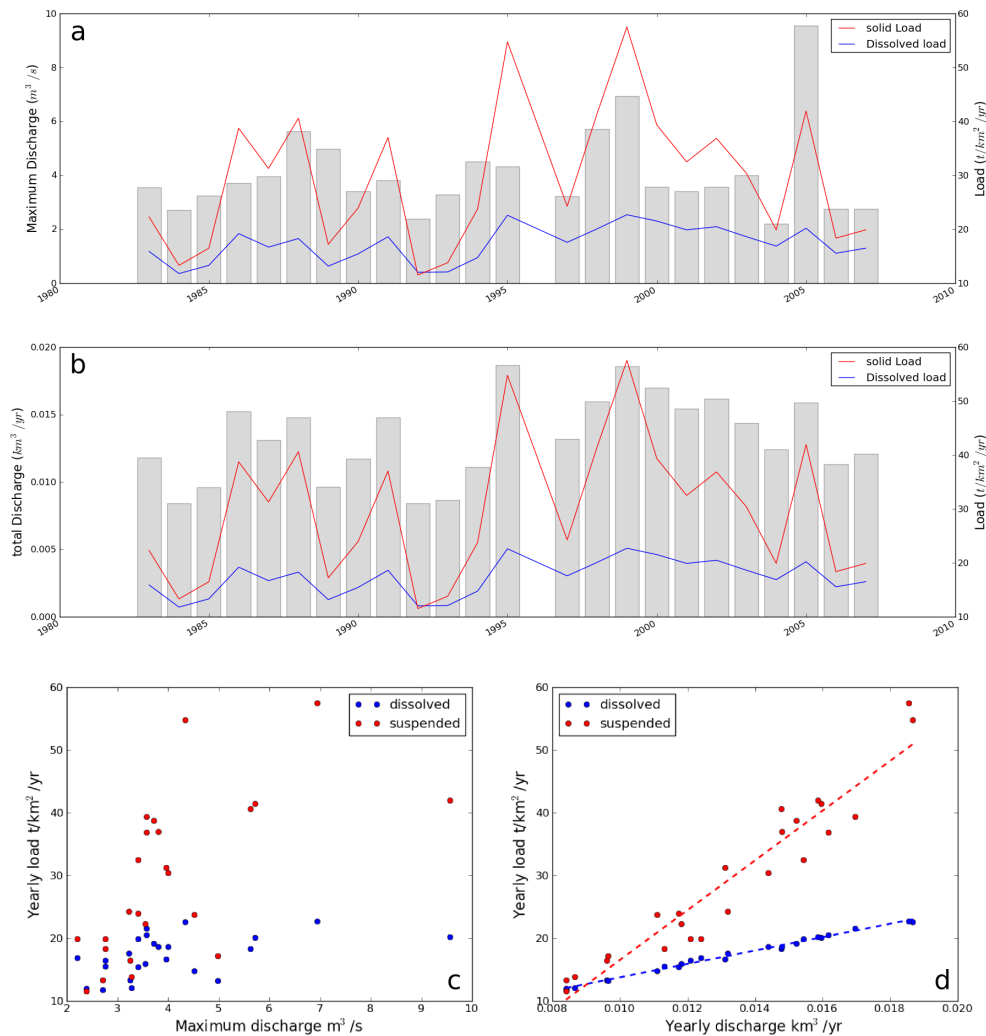


Fig. 13. Yearly Mass balance: **(a)** Calculated yearly chemical load and solid load in the Urumqi River during 24 years along with the maximum discharge recorded during the year. **(b)** Same plot but with the total discharge measured during the year. **(c)** Comparison between the yearly load and the maximum discharge recorded. **(d)** Comparison between the yearly load and the yearly discharge.

was $0.018^\circ\text{C yr}^{-1}$ over the range, with slightly lower values below an elevation of 2000 m. The precipitation in the Tianshan increased 1.2 mm yr^{-1} over the past half-century. The precipitation increase is larger at low altitudes in the northern and western regions than at altitudes above 2000 m (Aizen et al., 1997). Along the Urumqi River, there is a 19 % increase in the total annual precipitation but because of a significant increase in T, the glacial mass budget is negative and significant glacier retreat has occurred. Together with the increase in precipitation, this has induced a significant increase (62 %) in the total flow in the valley (Ye et al., 2005). In agreement with the hydrologic evolution, rates calculated during 1996–2006 are higher than then those of the preceding decade, yet there is a large amount of variance from one season to another.

From the integration of daily rates, it is also possible to see whether the sediment budget is controlled by the largest events recorded or by the total flow. Figure 13c–d are unambiguous. The correlation between mechanical or chemical weathering and yearly discharge is evident. By contrast the correlation with maximum yearly discharge is weak. It is then possible to derive a yearly correlation between both dissolved and mechanical weathering as follows:

$$W_d = 1067 Q + 3, R^2 = 0.99 \quad (16)$$

for yearly chemical denudation W_d and

$$W_m = 3966 Q - 23, R^2 = 0.91 \quad (17)$$

for the yearly mechanical denudation.

It is therefore possible to conclude that in the case of the Urumqi River, the yearly sediment transport budget (hence denudation) is essentially controlled by the total amount of water flowing and not by the largest floods.

6 Discussion

The most striking features of our survey on sediment transport along the Urumqi River are that (1) chemical weathering is not negligible. It accounts for a significant portion of the total weathering balance and carbonate weathering and atmospheric inputs are important controls on water chemistry. (2) The denudation rates we obtain are modest for such a high and tectonically active mountain range.

6.1 Chemical weathering and mechanical erosion

Chemical weathering is both consistent with the estimate of global average weathering rates (Goudie, 1995) and with other measurements of weathering fluxes in glacier-covered catchments (Prestrud Anderson et al., 1997). It lies well above the average fluxes of catchments underlain by granitoid rocks (Millot et al., 2002) but within the range of carbonate weathering fluxes (Calmels et al., 2011). In the Haut Glacier d'Arolla, chemical denudation is on the order of $40 \text{ t} \times \text{km}^{-2} \times \text{yr}^{-1}$ (Sharp et al., 1995), whereas silicate cation denudation rates were recently estimated to be approximately $18 \text{ t} \times \text{km}^{-2} \times \text{yr}^{-1}$ in Taiwan (Calmels et al., 2011). Finally, West et al. (2002) studied the weathering fluxes of four small Himalayan catchments. These catchments present a variety of settings from agricultural and forested to high Himalayan glacial catchments. Weathering fluxes vary from 13 to almost $40 \text{ t} \times \text{km}^{-2} \times \text{yr}^{-1}$. Chemical weathering in the Urumqi River therefore seems at pace with known observations of weathering in glacial environments. Carbonate weathering and sulphate oxidation are probably important because the headwater glaciers, although retreating, are still able to continuously refresh bedrock surfaces, thereby exposing these highly weatherable minerals.

On the contrary, the solid load (suspended and bed) is very low compared to other mountain settings. The denudation rate we obtain from our mass balance is small for an active mountain range. In the Karakoram, Bhutiyani (2000) studied the hydrology and sediment flux from the proglacial stream of the Siachen Glacier and found denudation rates of 300 to almost $1300 \text{ t} \times \text{km}^{-2} \times \text{yr}^{-1}$, i.e. between one and two orders of magnitude higher than in the Urumqi River. From a less constrained survey, Gabet et al. (2008) obtained rates of the same order of magnitude for the streams in the Annapurna watershed in Nepal. In the Swiss Alps, the study (Sharp et al., 1995) on the Haut Glacier d'Arolla reports suspended loads as high as $6300 \text{ t} \times \text{km}^{-2} \times \text{yr}^{-1}$. Finally, the rates we report here are orders of magnitude less than the $\sim 10\,000 \text{ t} \times \text{km}^{-2} \times \text{yr}^{-1}$ reported for Taiwan (Dadson et al., 2003).

As discussed in the preceeding sections, the hydrology of the Urumqi River is probably the main cause for this small solid load. Yet significant morphological differences, due for example to the inherited glacial morphology (in the case of the Urumqi River) or differences in active tectonics, could also explain these different rates.

In order to look for a possible influence of morphology, we compared the cumulative distribution functions of slopes in the Arolla, Annapurna, Kuitun, Siachen Urumqi and Taiwan island catchments morphologies. We used SRTM 4 or ASTER 2 DEMs when available to compare the distributions. Fig 14a shows the computed CDFs. A group of four catchments (Arolla, Annapurna, Kuitun, Urumqi) has comparable slope distributions for at least 60 % of their drainage area. Two catchments exhibit a clearly different slope distribution: Siachen and Taiwan. The Siachen catchment exhibits a very distinct trend because of the Siachen glacier that covers most of the catchment and has gentle surface slopes that are not corrected for in DEMs. Catchments in Taiwan island have significantly smaller slopes than the other catchments. It has to be noted also that the Annapurna catchment has more surface with high ($> 40^\circ$) slopes than the other catchments. As a simple and complementary way to graphically test the similarity in distribution functions of the slope datasets, we used Quantile-Quantile plots (QQ-plots). (NIST/SEMATECH, 2009; Métivier and Barrier, 2012). The quantiles of the slope CDFs for each catchments are compared to the corresponding quantiles of the slope distribution in our survey area (the Urumqi Glacial Valley). If the datasets are comparable (derived from the same distribution function), then the QQ-plots align on a 1:1 line. Figure 14b shows the result. Again Taiwan and Siachen, as expected, show a clear departure from the 1:1 correlation for low slopes. Let us note, though, that Siachen tends towards the 1:1 correlation for large slopes, hence above the glacier surface. The Quantiles of the Annapurna slope distribution departs from the 1:1 line correlation with the Urumqi for large slopes and, but to a lesser extent, for small slopes. The Quantiles of Arolla also show a slight departure for the largest slopes.

We are not aware of studies showing that erosion concentrates on the highest slopes of the Annapurna and Arolla basins and that this could be the reason why sediment load are higher in these catchments compared to the Urumqi River. Furthermore, the Taiwan catchments have much smaller slopes than the other one yet Taiwanese rivers carry the highest load. This therefore suggests that differences in slope distributions can probably not be advocated to explain the order of magnitude differences in reported loads in these rivers.

Tectonic uplift could also play a significant role. Unfortunately, Quaternary exhumation rates remain unknown in Tianshan. It is therefore impossible to compare with published exhumation rates in the western Himalayas (Zeitler, 1985; Foster et al., 1994) or in the Alps (Wittmann et al., 2007). At a much shorter timescale, contrary to Taiwan,

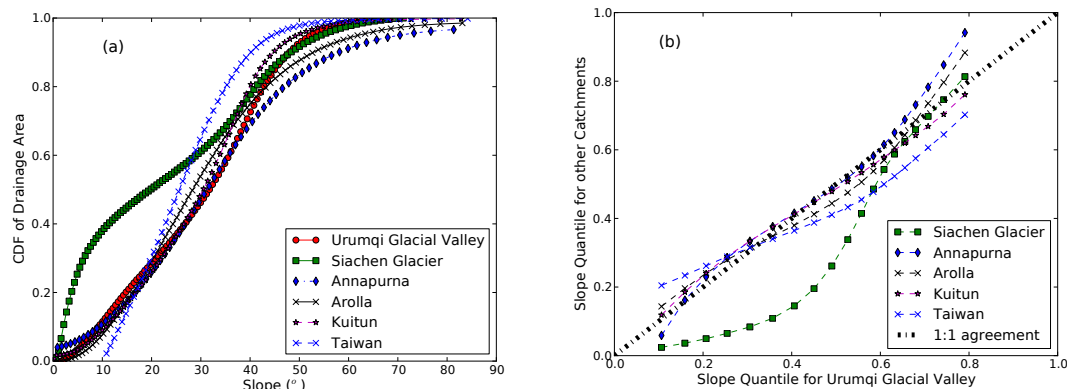


Fig. 14. (a) Cumulative distribution functions of slopes in the Arolla, Annapurna, Kuitun, Siachen and Urumqi catchments. (b) Quantile-Quantile plots of slope distribution in the Arolla, Annapurna, Kuitun and Siachen catchments compared to the Urumqi Glacial Valley catchment. Data derived from SRTM V4. and ASTER V2 DEMs. Tests were performed to ensure that the difference in grid spacing did not significantly bias the results. ASTER GDEM is a product of METI and NASA.

seismicity is probably not an issue in the case of the Annapurna, Arolla, Kuitun, Siachen and Urumqi catchments. For the Siachen and Annapurna catchments, the first $M > 6$ historical earthquakes recorded are almost 300 km away (National Geophysical Data Center/World Data Center (NGDC/WDC) Significant Earthquake Database, Boulder, CO, USA. (Available at <http://www.ngdc.noaa.gov/nndc/struts/form?t=101650&s=1&d=1>). In the case of the Urumqi River (if one excepts the Chinese $M \sim 6$ nuclear tests), there are nine $M > 6$ earthquakes below the same distance and two for the Arolla catchment. By contrast more than 30 earthquakes of $M \geq 6$ are reported in the NOAA catalogue within 300 km from the Taiwan island center. Thus, no picture emerges because catchments with high loads have experienced no large historical earthquakes (Annapurna), few (Arolla), or many (Taiwan); whereas the Urumqi River has experienced both historical and nuclear explosion earthquakes yet its load is small.

6.2 Present day rates of denudation

Thus, the mean denudation rate we estimate here is modest for a mountain range with peaks above 6000 m. It is also much smaller than the “present day” denudation rate of $\sim 500 \text{ m Myr}^{-1}$ obtained from river sand by Charreau et al. (2011) in the Kuitun River, a river that runs parallel and to the west of the Urumqi River.

The Kuitun River has more discharge than the Urumqi River and stands in a region where the amount of shortening is probably higher (Avouac et al., 1993; Charreau et al., 2011; Métivier and Gaudemer, 1997; Poisson and Avouac, 2004; Yang et al., 2008). Yet the difference between the present day denudation rates of the upper drainage of the Urumqi River and the rates obtained from the analysis of river sands on the Kuitun River is very large and remains to be explained.

One probable reason the rates found in the piedmont are higher is the reworking of glacial sediments stored in the floodplain. Sand samples dated by Charreau et al. (2011) were sampled downstream of the Kuitun River in its alluvial fan. They are supposed to integrate erosion on the entire catchment. Within this catchment, some regions may have low rates of erosion whereas others may have much higher rates. Our measurements were made along the headwater stream in the high range above an elevation of 3000 m. They are representative of erosion processes in the high range.

Therefore, if both measurements are correct and comparable from one drainage to the other, there must be a large increase of sediment flux down the rivers. It has been shown by Church and Slaymaker (1989) that the increase of sediment fluxes with the drainage area within a glaciated catchment could be attributed to the reworking of sediments accumulated during the Holocene in the river network. In northern Tianshan there is evidence attesting to a recent reworking of the sediment. The rivers (both Urumqi and Kuitun) are deeply entrenched in their Quaternary fans. This entrenchment goes back inside the drainage, as attested by fill-cut terraces in gorges upstream from the outlet of the range in the case of the Urumqi. Thus, although a proper mass balance remains to be performed, downstream of the Urumqi River or upstream of the Kuitun River, it is probable that the supposed higher rates of denudation found elsewhere at the front of the northern Tianshan are not representative of the present-day catchment scale denudation but of the reworking of past deposits stored in canyons and small sedimentary basins inside the range (Church and Slaymaker, 1989). The Houxia basin is an example of a small sedimentary braid plain along the Urumqi River that can serve as a temporary storage place.

6.3 Erosion and Tectonics

The rate found by Charreau et al. (2011) is of the same order of magnitude, or even higher, during the Quaternary. The reworking of sediments is more difficult to call to explain such rates. Métivier and Gaudemer (1997) performed a mass balance estimate of the fluxes accumulated in the sedimentary basins of Central Asia. The volumes reconstructed allow for a rough assessment of the denudation rates. The volume of coarse gravel, known as the Xiyu Formation, accumulated in the Dzunggar Basin amounts to $6 \pm 4 \times 10^3 \text{ km}^3$. The age of the base of this formation was traditionally assumed to be Quaternary (Métivier and Gaudemer, 1997), but as pointed out by Charreau et al. (2009), the formation is highly diachronous with ages ranging from 1 to 15 Ma. In the Dzunggar Basin, the ages reported by Charreau et al. (2009) to the west on the Kuitun River are on the order of 4.8–7.6 Ma. The drainage area of the northern Tianshan mountain that feeds the Dzunggar Basin is on the order of $25\,000 \text{ km}^2$. Assuming that all the sediments come from this area, this leads to long-term denudation rates on the order of $39 (+43/-18) \text{ m Myr}^{-1}$. Métivier and Gaudemer (1997) also estimated the volume of Pliocene accumulation to be on the order of $48 \pm 18 \times 10^3 \text{ km}^3$. These deposits are generally attributed to the upper Dushanzi Formation (e.g. Charreau et al., 2009; Métivier and Gaudemer, 1997) and can most often, but probably not always, be distinguished from the Xiyu gravel. We can therefore use this volume to derive an upper bound to the denudation rates in northern Tianshan during the Upper-Pliocene and Quaternary. By assuming that the entire volume corresponds to the Xiyu Formation, we then obtain a maximum denudation rate on the order of $348 (+285/-180) \text{ m Myr}^{-1}$.

To conclude, long-term denudation rate obtained from a mass balance or sediment accumulated in the Dzunggar basin is closer to our short-term “upstream” denudation rate than the “downstream” rate found by Charreau et al. (2011). However, by using the largest possible volume accumulated in the Dzunggar Basin, we show that this latter rate of denudation of several hundreds of meters per million year is still possible.

Solving for the integration time scale of the denudation rates in Tianshan is important because it has geodynamic implications. Avouac and Burov (1996) have shown that, depending on the strain rate and erosion rates inside a mountain range like Tianshan, several scenarios could be imagined. For a given strain rate, the range will undergo subsurface collapse if erosion rates are small. The range will grow and develop some form of dynamic equilibrium if rates of erosion are balanced by inward flux of material and isostatic compensation. Finally an erosional collapse should develop if convergence and inward flux cannot balance the erosion rates. Most of the attention has been focused on the mountain growth regime (e.g. Whipple, 2009) because the interplay between tectonics and erosion has been studied in re-

gions of both rapid convergence and high erosion rate due to very humid conditions. In regions such as Central Asia where rainfall is essentially orogenic and much lower than in the Himalayas, for instance, our study and long-term denudation rates would indicate that the Tianshan mountain range is more probably in a regime where there is no dynamic equilibrium between denudation and uplift. Hence, if shortening continues, subsurface collapse, which has yet not been observed, should occur. On the contrary, high rates such as the one Charreau et al. (2011) presented, would probably be enough to keep the range in a mountain growth regime, as already stated by Avouac and Burov (1996, figure 12, p. 17761).

7 Conclusions

Our survey of the Urumqi River enables us to draw several conclusions regarding the dynamics of erosion and sediment transport in the high mountains of Tianshan. (1) Robust estimates of denudation rates can be performed using classical procedures. Rating curves can be obtained that, when coupled to long-term surveys of discharge, enable to assess long secular denudation rates. (2) We have shown that dissolved load accounted for almost half of the total load. Chemical weathering reactions in the Urumqi River are caused by the cation of carbonic and sulphuric acids (with about the same contribution). Due to the heavy ion concentration of Central Asian rainfalls, chemical weathering is of less importance but still accounts for one third of the total denudation of this glacierized catchment. It is important to outline the importance of atmospheric inputs in basins such as the upper Urumqi River. These atmospheric inputs are derived from the weathering of mineral present in the atmosphere and not produced locally. Future studies should focus on dry deposition, which may represent a significant role, particularly in low weathering regimes. Estimating the weathering rate in such an environment requires the knowledge of the precipitation input that is likely to change with time. (3) Significant bed load occurs during the entire flow season. Bed load amounts to 30–40 % of the solid load and is therefore important to quantify. Further study of bed load is needed, as, by virtue of the sizes in movement, it may bring some more insight into local transport and erosion mechanisms. It is also important to study bed load dynamics given that river sand in the Urumqi River moves as bedload and not as suspended load. Therefore, the assumptions used to derive denudation rates from the cosmogenic dating of river sand heavily relies on the poorly constrained dynamics of bed load transport. (4) Analysis of the hydrology shows that denudation is not driven by large infrequent events but controlled by the total yearly amount of rainfall, in contrast to what has been found in much more humid settings. (5) These results show that the erosion-driven evolution of mountain ranges that has gained wide acceptance in recent years based on studies performed

in the Himalayas, Taiwan and other highly humid ranges may not apply to semi-arid settings such as those that prevail in the mountains of Central Asia. Further work is especially needed to explain why present-day rates are in agreement with Plio-Quaternary rates and at more than an order of magnitude lower than rates inferred from cosmogenic isotopes. Our results clearly show the importance of studying sediment transport dynamics at different space and time scales as well as in different climate settings.

Supplementary material related to this article is available online at:

<http://www.solid-earth.net/2/283/2011/se-2-283-2011-supplement.zip>

Acknowledgements. The research program on the Urumqi River was funded by the French Programme de Recherches Avancées (PRA-T05), ANR-09-RISK-004/GESTRANS and INSU RELIEF grants to F. Métivier, by the French Ministry of Foreign Affairs (PhD thesis grant to Liu), National Basic Research Program of China (973 Program, grant 2007CB411502 to B. Ye) and Distinguished scholar of the 100-Talent program of Chinese Academy of Sciences (40871036 to B. Ye). Caroline Gorge performed the chemical analyses. Editorial assistance was provided by Sara Mullin. The manuscript benefitted from the constructive comments of A. Crave, A. Galy and M. Jolivet. This is IPGP contribution 3193.

Edited by: A. Galy

References

- Aizen, V., Aizen, E., Melack, J., and Dozier, J.: Climatic and hydrologic changes in the Tien Shan, central Asia, *J. Climate*, 10, 1393–1404, 1997.
- Anderson, S., Longacre, S., and Kraal, E.: Patterns of water chemistry and discharge in the glacier-fed Kennicott River, Alaska: evidence for subglacial water storage cycles, *Chem. Geol.*, 202, 297–312, 2003.
- Ashworth, P. J., Fergusson, R. I., Ashmore, P. E., Paola, C., Powell, D. M., and Prestegard, K. L.: Measurements in a braided river chute and lobe 2. Sorting of bed load during entrainment, transport and deposition, *Water Resour. Res.*, 28, 1887–1896, 1992.
- Avouac, J. P. and Tapponnier, P.: Kinematic model of active deformation in central Asia, *Geophys. Res. Lett.*, 20, 895–898, 1993.
- Avouac, J. P. and Burov, E. B.: Erosion as a driving mechanism of intracontinental mountain growth, *J. Geophys. Res.*, 101, 17747–17769, 1996.
- Avouac, J. P., Tapponnier, P., Bai, M., You, H., and Wang, G.: Active thrusting and folding along the northern Tien Shan and late Cenozoic rotation of the Tarim relative to Dzungaria and Kazakhstan, *J. Geophys. Res.*, 98B4, 6655–6804, 1993.
- Bennis, S.: *Hydraulique et Hydrologie*, Presses de l'université du Québec, 2007.
- Berner, E. and Berner, R.: *Global environment: Water, air and geochemical cycles*, Prentice Hall, 1996.
- Bhutiya, M.: Sediment load characteristics of a proglacial stream of Siachen Glacier and the erosion rate in Nubra valley in the Karakoram Himalayas, India, *J. Hydrol.*, 227, 84–92, 2000.
- Blum, J., Gazis, C., Jacobson, A., and Page Chamberlain, C.: Carbonate versus silicate weathering in the Raikhot watershed within the High Himalayan Crystalline Series, *Geology*, 26, 411–414, 1998.
- Bunte, K. and Abt, S.: Effect of sampling time on measured gravel bed load transport rates in a coarse-bedded stream, *Water Resour. Res.*, 41, W11405, doi:10.1029/2004WR003880, 2005.
- Bunte, K., Abt, S., Potyondy, J., and Swingle, K.: A comparison of coarse bedload transport measured with bedload traps and Helley-Smith samplers, *Geodin. Acta*, 21, 53–66, 2008.
- Caine, N.: Spatial patterns of geochemical denudation in a Colorado alpine environment, *Periglacial Geomorphology*, edited by J. C. Dixon and A. B. Abrahams, Wiley, Chichester, 63–88, 1992.
- Calmels, D., Gaillardet, J., Brenot, A., and France-Lanord, C.: Sustained sulfide oxidation by physical erosion processes in the Mackenzie River basin: Climatic perspectives, *Geology*, 35, 1003–1006, doi:10.1130/G24132A.1, 2007.
- Calmels, D., Galy, A., Hovius, N., Bickle, M., West, A. J., Chen, M.-C., and Chapman, H.: Contribution of deep groundwater to the weathering budget in a rapidly eroding mountain belt, Taiwan, *Earth Planet. Sc. Lett.*, 303, 48–58, doi:10.1016/j.epsl.2010.12.032, 2011.
- Charreau, J., Gumiaux, C., Avouac, J., Augier, R., Chen, Y., Barrier, L., and Gilder, S.: The Neogene Xiyu Formation, a diachronous prograding gravel wedge at front of the Tianshan: Climatic and tectonic implications, *Earth Planet. Sc. Lett.*, 287, 298–310, 2009.
- Charreau, J., Blard, P., Puchol, N., Avouac, J., Lallier-Vergès, E., Bourlès, D., Braucher, R., and Gallaud, A.: Paleo-erosion rates in Central Asia since 9 Ma: A transient increase at the onset of Quaternary glaciations?, *Earth Planet. Sc. Lett.*, 304, 85–92, doi:10.1016/j.epsl.2011.01.018, available at: <http://www.sciencedirect.com/science/article/pii/S0012821X11000422>, 2011.
- Church, M. and Slaymaker, O.: Disequilibrium of Holocene sediment yield in glaciated British Columbia, *Nature*, 337, 452–454, 1989.
- Dadson, S. J., Hovius, N., Chen, H., Dade, W. B., Hsieh, M. L., Willett, S. D., Hu, J. C., Horng, M. J., Chen, M. C., Stark, C. P., Lague, D., and Lin, J. C.: Links between erosion, runoff variability and seismicity in the Taiwan orogen, *Nature*, 426, 648–651, 2003.
- Devauchelle, O., Métivier, F., Lajeunesse, E., Gaillardet, J., Liu, Y., and Ye, B.: Dissolution in a porous medium: effect on the concentration – discharge relationships, in: *River, Coastal and Estuarine Morphodynamics 2011*, IAHR, 2011.
- Dietrich, W. E., Bellugi, D. G., Sklar, L. S., Stock, J. D., Heimsath, A., and Roering, J.: geomorphic transport law for predicting landscape form and dynamics, in: *Prediction in Geomorphology*, 135, 1–30, 2003.
- Diplas, P., Kuhnle, R., Gray, J., Glysson, D., and Edwards, T.: Sediment transport measurements, in: *Sedimentation engineering: processes, management, modeling, and practice*, edited by: Garcia, M. H., 110(5), 307–353, ASCE, 2008.
- Foster, D., Gleadow, A., and Mortimer, G.: Rapid Pliocene exhumation in the Karakoram (Pakistan), revealed by fission-track ther-

- mochronology of the K2 gneiss, *Geology*, 22, 19, 1994.
- Gabet, E., Burbank, D., Pratt-Sitaula, B., Putkonen, J., and Bookhagen, B.: Modern erosion rates in the High Himalayas of Nepal, *Earth Planet. Sc. Lett.*, 267, 482–494, 2008.
- Galy, A. and France-Lanord, C.: Higher erosion rates in the Himalaya: Geochemical constraints on riverine fluxes, *Geology*, 29, 23–26, 2001.
- Godsey, S., Kirchner, J., and Clow, D.: Concentration–discharge relationships reflect chemostatic characteristics of US catchments, *Hydrol. Process.*, 23, 1844–1864, 2009.
- Goudie, A.: *The changing earth*, Blackwell, 1995.
- Habersack, H., Seitz, H., and Laronne, J. B.: Spatio-temporal variability of bedload transport rates, *Gedimica acta*, 21, 67–78, 2008.
- Han, T., Ding, Y., Ye, B., Liu, S., and Jiao, K.: Mass-balance characteristics of Urumqi glacier No. 1, Tien Shan, China, *Ann. Glaciol.*, 43, 323–328, 2006.
- Howard, A. D., Dietrich, W. E., and Seidl, M. A.: Modeling fluvial erosion on regional to continental scales, *JGR*, 99, 13971–13986, 1994.
- Hubbell, D. W.: Bed load sampling and analysis, in: *Sediment transport in gravel bed rivers*, edited by: Thorne, C. R., Bathurst, J. C., and Hey, R. D., 89–106, John Wiley and Sons Ltd., Chichester, 1987.
- Jacobson, A. and Blum, J.: Ca/Sr and $^{87}\text{Sr}/^{86}\text{Sr}$ geochemistry of disseminated calcite in Himalayan silicate rocks from Nanga Parbat: Influence on river-water chemistry, *Geology*, 28, 463–466, 2000.
- Kuhnle, R.: Bed Load transport during rising and falling stages on two small streams, *Earth. Surf. Process. Landforms*, 17, 191–197, 1992.
- Lague, D., Crave, A., and Davy, P.: Laboratory experiments simulating the geomorphic response to tectonic uplift, *J. Geophys. Res.*, 108(B1), 2008, doi:10.1029/2002JB001785, 2003.
- Lee, X., Qin, D., Hou, S., Ren, J., Duan, K., and ZHou, H.: Changes in chemical and isotopic properties near infiltrated cracks in an ice core from Urumqi glacier No. 1, Tien Shan, China, *Ann. Glaciol.*, 35, 162–166, 2002.
- Lenzi, M., Mao, L., and Comiti, F.: Interannual variation of suspended sediment load and sediment yield in an alpine catchment, *Hydrolog. Sci. J.*, 48, 899–916, 2003.
- Li, Z., Edwards, R., Mosley-Thompson, E., Wang, F., Dong, Z., You, X., Li, H., Li, C., and Zhu, Y.: Seasonal variability of ionic concentrations in surface snow and elution processes in snowfirn packs at the PGPI site on Urumqi glacier No. 1, eastern Tien Shan, China, *Ann. Glaciol.*, 43, 250–256, 2006.
- Li, Z., Wang, W., Zhang, M., Wang, F., and Li, H.: Observed changes in streamflow at the headwaters of the Urumqi River, eastern Tianshan, central Asia, *Hydrol. Process.*, 24, 217–224, 2010.
- Liu, F., Williams, M., and Yang, D.: Snow and water chemistry of a headwater alpine basin, Urumqi River, Tian Shan, PR China, in: *Biogeochemistry of seasonally snow covered catchments*, edited by: Williams, M. and Tranter, M., IAHS-AIHS Publ. 228, 1995.
- Liu, Y., Métivier, F., Lajeunesse, E., Lancien, P., Narteau, C., and Meunier, P.: Measuring bed load in gravel bed mountain rivers: averaging methods and sampling strategies, *Geodynamica Acta*, 21, 81–92, 2008.
- Liu, Y., Métivier, F., Ye, B., Narteau, C., Han, T., and Meunier, P.: Relationship between Streambed Evolution and Runoff in Gravel-bed Streams, Urumqi River, in: *2nd International Conference on Information Science and Engineering (ICISE2010)*, 2010.
- Métivier, F. and Barrier, L.: Alluvial landscape evolution: what do we know about metamorphosis of gravel bed meandering and braided streams, in: *Gravel-bed Rivers: processes, tools, environments.*, edited by: Church, M., Biron, P., and Roy, A., 34, 474–501, Wiley & Sons, Chichester, 2012.
- Métivier, F. and Gaudemer, Y.: Mass transfer between eastern Tien Shan and adjacent basins (central Asia): Constraints on regional tectonics and topography, *Geophys. J. Int.*, 128, 1–17, 1997.
- Métivier, F. and Gaudemer, Y.: Stability of output fluxes of large rivers in South and East Asia during the last 2 million years: implications on floodplain processes, *Basin Res.*, 11, 293–303, 1999.
- Métivier, F., Meunier, P., Moreira, M., Crave, A., Chaduteau, C., Ye, B., and Liu, G.: Transport dynamics and morphology of a high mountain stream during the peak flow season: the Urumqi river (Chinese Tian-Shan), in: *Second international conference on fluvial hydraulics – River flow 2004*, 2004.
- Meunier, P., Métivier, F., Lajeunesse, E., Meriaux, A. S., and Faure, J.: Flow pattern and sediment transport in a braided river: The torrent de St Pierre (French Alps), *J. Hydrol.*, 330, 496–505, doi:10.1016/j.jhydrol.2006.04.009, available at: <http://dx.doi.org/10.1016/j.jhydrol.2006.04.009>, 2006a.
- Meunier, P., Métivier, F., Lajeunesse, E., Meriaux, A. S., and Faure, J.: Flow pattern and sediment transport in a braided river: The “torrent de St Pierre” (French Alps), *J. Hydrol.*, 330, 496–505, 2006b.
- Millot, R., Gaillardet, J., Dupré, B., and Allègre, C.: The global control of silicate weathering rates and the coupling with physical erosion: new insights from rivers of the Canadian Shield, *Earth Planet. Sc. Lett.*, 196, 83–98, 2002.
- Molnar, P., Thorson Brown, E., Burchfiel, B. C., Deng, Q., Feng, X., Li, J., Raisbeck, M., Shi, J., Wu, Z., Yiou, F., and You, H.: Quaternary climate change and the formation of river terraces across growing anticlines on the north flank of the Tien Shan area, *J. of Geology*, 102, 583–602, 1994.
- Mueller, E. R. and Pitlick, J.: Morphologically based model of bed load transport capacity in a headwater stream, *J. Geophys. Res.*, 110, F02016 doi:10.1029/2003JF000117, 2005.
- Negrel, P., Allegre, C., Dupré, B., and Lewin, E.: Erosion sources determined by inversion of major and trace element ratios and strontium isotopic ratios in river water: The Congo Basin case, *Earth Planet. Sc. Lett.*, 120, 59–76, 1993.
- NIST/SEMATECH: e-Handbook of Statistical Methods, <http://www.itl.nist.gov/div898/handbook/>, 2009.
- Oliva, P., Viers, J., Dupré, B., Fortuné, J. P., Martin, F., Braun, J. J., Nahon, D., and Robain, H.: The effect of organic matter on chemical weathering: study of a small tropical watershed: nsimi-zoétéélé site, cameroon, *Geochim. Cosmochim. Ac.*, 63, 4013–4035, doi:10.1016/S0016-7037(99)00306-3, available at: <http://www.sciencedirect.com/science/article/pii/S0016703799003063>, 1999.
- Paola, C., Heller, P. L., and Angevine, C. L.: The large-scale dynamics of grain-size variation in alluvial basins, 1: Theory, *Basin Res.*, 4, 73–90, 1992.
- Pelpola, C. and Hickin, E.: Long-term bed load transport rate based

- on aerial-photo and ground penetrating radar surveys of fan-delta growth, Coast Mountains, British Columbia, *Geomorphology*, 57, 169–181, 2004.
- Pitlick, J., Segura, C., and Mueller, E. R.: Influence of sediment transport intensity and hydrology on the bankfull hydraulic geometry of gravel bed rivers, *EOS Transactions of the American Geophysical Union*, 2010.
- Poisson, B. and Avouac, J. P.: Holocene hydrological changes inferred from alluvial stream entrenchment in North Tian Shan (Northwestern China), *J. Geol.*, 112, 231–249, 2004.
- Pratt-Sitaula, B., Garde, M., Burbank, D., Oskin, M., Heimsath, A., and Gabet, E.: Bedload-to-suspended load ratio and rapid bedrock incision from Himalayan landslide-dam lake record, *Quaternary Res.*, 68, 111–120, 2007.
- Prestrud Anderson, S., Drever, J., and Humphrey, N.: Chemical weathering in glacial environments, *Geology*, 25, 399–402, 1997.
- Riebe, C., Kirchner, J., Granger, D., and Finkel, R.: Strong tectonic and weak climatic control of long-term chemical weathering rates, *Geology*, 29, 511, 2001.
- Ryan, S. E. and Porth, L. S.: A field comparison of three pressure-difference bedload sampler, *Geomorphology*, 30, 307–322, 1999.
- Sanders, L.: A manual of field hydrogeology, Prentice-Hall, Inc., 113 Sylvan Ave. Englewood Cliffs NJ 07632 USA, 381, 1998 pp., 1998.
- Schiefer, E., Hassan, M., Menounos, B., Pelpola, C., and Slaymaker, O.: Interdecadal patterns of total sediment yield from a montane catchment, southern Coast Mountains, British Columbia, Canada, *Geomorphology*, 118, 207–212, 2010.
- Sharp, M., Tranter, M., Brown, G. H., and Skidmore, M.: Rates of chemical denudation and CO₂ drawdown in a glacier-covered alpine catchment, *Geology*, 23, 61–64, 1995.
- Smith, D.: Long-term rates of contemporary solifluction in the Canadian Rocky Mountains, *Periglacial Geomorphology*, edited by: J. C. Dixon and Abrahams, A. B., Wiley, Chichester, 203–221, 1992.
- Thomas, R. and Lewis, J.: A new model for bed load sampler calibration to replace the probability-matching method, *Water Resour. Res.*, 29, 583–597, 1993.
- Turowski, J. M., Rickenmann, D., and Dadson, S. J.: The partitioning of the total sediment load of a river into suspended load and bedload: a review of empirical data, *Sedimentology*, 57, 1126–1146, 2010.
- Vericat, D., Church, M., and Batalla, R.: Bed load bias: Comparison of measurements obtained using two (76 and 152) helley-Smith samplers in a gravel bed river, *Water Resour. Res.*, 42, W01402, doi:10.1029/2005WR004025, available at: <http://dx.doi.org/10.1029/2005WR004025>, 2006.
- Wang, Q., Zhang, P. Z., Freymueller, J. T., Bilham, R., Larson, K. M., Lai, X., You, X., Niu, Z., Wu, J., Li, Y., Liu, J., Yang, Z., and Chen, Q.: Present-day Crustal Deformation in China Constrained by Global Positioning System Measurements, *Science*, 294, 574–577, 2001.
- West, A., Bickle, M., Collins, R., and Brasington, J.: Small-catchment perspective on Himalayan weathering fluxes, *Geology*, 30, 355–358, 2002.
- West, A. J., Galy, A., and Bickle, M.: Tectonic and climatic controls on silicate weathering, *Earth Planet. Sc. Lett.*, 235, 211–228, doi:10.1016/j.epsl.2005.03.020, available at: <http://www.sciencedirect.com/science/article/pii/S0012821X05002116>, 2005.
- Whipple, K.: The influence of climate on the tectonic evolution of mountain belts, *Nat. Geosci.*, 2, 97–104, 2009.
- Williams, M. W., Yang, D., Liu, F., Turk, J., and M., M. J.: Controls on the major ion chemistry of the Ürümqi River, Tian Shan, People's Republic of China., *J. Hydrol.*, 172, 209–229, 1995.
- Wittmann, H., von Blanckenburg, F., Kruesmann, T., Norton, K., and Kubik, P.: Relation between rock uplift and denudation from cosmogenic nuclides in river sediment in the Central Alps of Switzerland, *J. Geophys. Res.*, 112, 2007.
- Wulf, H., Bookhagen, B., and Scherler, D.: Seasonal precipitation gradients and their impact on fluvial sediment flux in the North-west Himalaya, *Geomorphology*, 118, 13–21, 2010.
- Yang, S., Jie, L., and Wang, Q.: The deformation pattern and fault rate in the Tianshan Mountains inferred from GPS observations, *Science in China series D: Earth Sci.*, 51, 1064–1080, 2008.
- Ye, B., Ding, Y., Liu, F., and Liu, C.: Responses of various-sized alpine glaciers and runoff to climatic change, *J. Glaciol.*, 49, 1–7, 2003.
- Ye, B., Yang, D., Jiao, K., Han, T., Jin, Z., Yang, H., and Li, Z.: The Urumqi River source glacier No. 1, Tianshan, China: changes over the past 45 years, *Geophys. Res. Lett.*, 32, L21504, doi:10.1029/2005GL024178, 2005.
- Yi, C., Jiao, K., Liu, K., He, Y., and Ye, Y.: ESR dating of the sediments of the Last Glaciation at the source area of the Urumqi River, Tian Shan Mountains, China, *Quatern. Int.*, 97, 141–146, 2002.
- Zeitler, P.: Cooling history of the NW Himalaya, Pakistan, *Tectonics*, 4, 127–151, 1985.
- Zhang, W., Chen, J., Ogawa, K., and Yamaguchi, Y.: An approach to estimating evapotranspiration in the Urumqi River basin, Tianshan, China, by means of remote sensing and a geographical information system technique, *Hydrol. Processes*, 19, 1839–1854, 2005.
- Zhao, Z., Tian, L., Fischer, E., Li, Z., and Jiao, K.: Study of chemical composition of precipitation at an alpine site and a rural site in the Urumqi River Valley, Eastern Tien Shan, China, *Atmos. Environ.*, 42, 8934–8942, 2008.